Available online at www.sciencedirect.com
SCIENCE DIRECT®
International Journal of Pharmaceutics 273 (2004) 9–22
international journal of pharmaceutics
www.elsevier.com/locate/ijpharm

Mechanistic studies of flux variability of neutral and ionic permeants during constant current dc iontophoresis with human epidermal membrane

S. Kevin Li*, William I. Higuchi, Rajan P. Kochambilli, Honggang Zhu

Pharmaceutics and Pharmaceutical Chemistry, University of Utah, 30 S 2000 E, Rm 213 Skaggs Hall, Salt Lake City, UT 84112, USA

Received 17 September 2003; received in revised form 10 December 2003; accepted 11 December 2003

Abstract

Although constant current iontophoresis is supposed to provide constant transdermal transport, significant flux variability and/or time-dependent flux drifts are observed during iontophoresis with human skin in vitro and human studies in vivo. The objectives of the present study were to determine (a) the causes of flux variability in constant current dc transdermal iontophoresis and (b) the relationships of flux variabilities among permeants of different physicochemical properties. Changes in the human epidermal membrane (HEM) effective pore size and/or electroosmosis during constant current dc iontophoresis were examined. Tetraethylammonium ion (TEA), urea, and mannitol were the model permeants. For the neutral permeants, the results in the present study showed a significant increase of fluxes with time in a given experiment and large HEM sample-to-sample variability. Although both effective pore size and pore charge density variations contributed to the time-dependent flux drifts observed in electroosmotic transport, the significant flux drifts observed were found to be primarily a result of the time-dependent increase in effective pore charge density. For the ionic permeant, the observed flux variability was smaller than that of the neutral permeants and was believed to be primarily due to effective pore size alteration in HEM during iontophoresis as suggested in a previous study. The different extents of flux variability observed between neutral and ionic permeants are consistent with the different iontophoretically enhanced transport mechanisms for the neutral and ionic permeants (i.e. electroosmosis and electrophoresis, respectively). The results of the present study also demonstrate that flux variability of two neutral permeants are inter-related, so the flux of one neutral permeant can be predicted if the permeability coefficient of the other neutral permeant is known.

Keywords: Transdermal; Iontophoresis; Electroosmosis; Flux variability; Human epidermal membrane

1. Introduction

Constant current dc iontophoresis theoretically provides a constant, predictable, and programmable rate of transdermal transport that is only dependent upon the applied current. However, large flux variabilities are often observed in iontophoretic transport (e.g. Singh et al., 1995; Chang et al., 2000; Lopez et al., 2001; Nicoli et al., 2001; Smyth et al., 2002; Zhu et al., 2002; Li et al., 2003). These variabilities include inter-sample variability and/or time-dependent flux drifts. The practical significance of such variabilities in transdermal iontophoresis can be considerable. An example is the problem caused by flux variability in the FDA approved iontophoretic non-invasive glucose monitoring system. This system requires a "warm

* Corresponding author. Tel.: +1-801-581-4110; fax: +1-801-585-1270.
E-mail address: kevin.li@m.cc.utah.edu (S.K. Li).

0378-5173/$ – see front matter © 2004 Elsevier B.V. All rights reserved.
doi:10.1016/j.ijpharm.2003.12.009

up" period followed by a calibration which involves establishing a correlation with a traditional blood glucose monitoring device (Tamada et al., 1999; Tierney et al., 2001). The need for such requirements reflects the present state of iontophoretic glucose monitoring and the need for better understanding transdermal iontophoresis in general so that the technology may be significantly improved.

The variability of passive skin permeation data of ionic and neutral permeants has been previously investigated (Liu et al., 1993), but the causes of flux variability during constant current dc iontophoresis are not well understood. Iontophoretic transport is related to the properties of the permeant, the membrane, and the surrounding solution. When the membrane properties and the surrounding solution are maintained constant in an experiment, constant current should provide constant permeant flux with little flux variability. It is believed that the observed flux variability during iontophoresis is a result of the alterations of the membrane properties under the electric field that have different effects upon the transport of the background electrolyte ions and the permeant of interest (Zhu et al., 2001). Particularly, the electric field can induce pore formation and the pores can have different sizes and different surface charge densities than those of the pre-existing pores, changing the distribution of the effective pore size and effective pore charge in the stratum corneum. A key question in the present study is: what is the extent of the changes of the effective pore size in the stratum corneum and the pore-charge related electroosmosis during constant current dc iontophoresis?

The objectives of present study were (a) to determine the mechanisms of flux variability during constant current dc iontophoresis of ionic permeants and polar non-electrolytes with human epidermal membrane (HEM) and (b) to test for possible relationships between flux variabilities of ionic and neutral permeants. Tetraethylammonium ion (TEA), mannitol, and urea were the model permeants in this study. Experiments were designed to examine (a) the time-dependent changes in effective pore size and/or pore charge density and the related time-dependent flux drifts within an iontophoresis run and (b) inter-sample variability during iontophoresis. Understanding the alteration in HEM barrier properties during iontophoresis and the mechanisms of flux variability could help pharmaceutical researchers better predict permeant flux during constant current dc transdermal iontophoresis. Such an understanding would also allow the use of the flux of one permeant to predict the flux of another permeant during iontophoresis.

2. Materials and methods

2.1. Materials

Phosphate-buffered saline (PBS), pH 7.4 and 0.1 M ionic strength, were prepared with reagent grade chemicals and deionized water (>10 MΩ) processed by a Milli-Q reagent water system. Sodium azide (NaN_3, 0.02%) was added into PBS as a bacteriostatic agent. Millipore SCWP filters (8 μm pore diameter) were purchased from Millipore Corp. (Bedford, MA). [^{3}H]mannitol (15–30 Ci/mmol), [^{14}C]mannitol (45–60 mCi/mmol), [^{14}C]urea (40–60 mCi/mmol), and [^{14}C]TEA (2–5 mCi/mmol) were purchased from New England Nuclear (Boston, MA) and Moravek Biochemicals (Brea, CA) and their purity was checked to be at least 98%. Dextran sulfate (average MW 500,000) was purchased from Sigma Chemicals (St. Louis, MO). All materials were used as received unless noted otherwise.

2.2. Experimental strategies

Iontophoretic transport of ionic permeants such as TEA is expected to take place predominantly via the same pathways as the conducting background electrolyte ions (Phipps and Gyory, 1992; Zhu et al., 2001). Because transport by electroosmosis in HEM has been well established to be around or less than 10% of electrophoresis for small permeants (MW < 400; Sims et al., 1991; Peck et al., 1996; Bath et al., 2000; Marro et al., 2001; Zhu et al., 2001) and because the effects of pore charge upon the partitioning of ionic permeants into the charged pores have been shown not to be significant at ionic strengths of 0.1 M for HEM (Peck et al., 1993), the variation in effective HEM pore size is expected to be the principal factor responsible for the flux variability observed with TEA during constant current dc iontophoresis. Iontophoretically enhanced transport of polar non-electrolytes such as urea and

mannitol is mainly due to electroosmosis. Unlike TEA for which changes in the effective pore size alone during constant current iontophoresis are expected to account for the flux variability during iontophoresis, the situation for polar neutral permeants is more complicated: changes in both effective pore size and effective pore charge density are expected to be important in the interpretation and prediction of flux variability during iontophoresis.

To investigate flux variability based on HEM effective pore size and effective pore charge, the present study was divided into three parts: PBS as the background electrolyte with mannitol and TEA as permeants, PBS as the background electrolyte with mannitol and urea as permeants, and sodium ion as the only current carrier in HEM with mannitol and urea as permeants. Constant current dc experiments with TEA were to provide data for the assessment of flux variability due to effective pore size alteration of HEM, and experiments with mannitol were to provide data for the electroosmosis pathways in HEM during iontophoresis. Comparisons between the flux variability of mannitol and that of TEA, permeants of essentially the same molecular size (Table 1) but of different transport mechanisms (TEA carries a positive charge), were to permit a comparative examination of flux variabilities due to electroosmosis and electrophoresis. Experiments with mannitol and urea were to assess the effective pore size and pore charge of the negatively charged pores in HEM electroosmosis and their relationships to flux variability. Mannitol also has a molecular size and physicochemical properties similar to those of glucose, an important marker for diabetic management (e.g. Sieg et al., 2003). Urea is also endogenous, that is available in the body, and can be a therapeutic marker (e.g. Degim et al., 2003). In the last set of experiments, high molecular weight dextran sulfate was to be the only background electrolyte in the receiver solution at the cathode, so sodium ions would be the only current carrier. These experiments would permit examining the effects of different background electrolyte ion sizes (i.e. sodium plus chloride ions versus sodium ions only) upon flux variability by comparing the flux variabilities in the experiments of dextran sulfate and those of PBS. In these experiments, mannitol and urea were again to be the model permeants. It should be noted that due to the nature of the experimental design in the present study, caution must be exercised in extrapolating conclusions from the present study to permeants of different molecular weights. The permeant transport behavior with HEM probed in the present analysis and any of the conclusions may be limited to the model permeants chosen in the present study.

Table 1
Diffusion coefficients and radii of permeant and background electrolyte ions at 37 °C

Permeant	Diffusion coefficient ($\times 10^{-5}$ cm^2/s)	Radius (Å)
Na^+	1.78[a]	2.5[a,b]
Cl^-	2.72[a]	1.9[a,b]
TEA^+	1.07[a]	3.6[a,b]
Urea	1.75[c]	2.7[b,c]
Mannitol	0.90[c]	4.1[a,b]

[a] Data from Zhu et al. (2001); diffusion coefficient is calculated using the relationship: $zFD = uR_{gas}T$, where u is the electromobility at infinite dilution (Lide, 1990), z is the valence of charge, R_{gas} is the gas constant, T is the temperature, and F is the Faraday's constant. The diffusion coefficient of TEA determined using this method was consistent with that obtained in permeation experiments with a fritted glass disc and side-by-side diffusion cell as described in Peck et al. (1994).

[b] Hydrated radius (r_s) is calculated using the method described by Beck and Schultz (1972):

$$r_s = \left(1.5 \times \frac{R_w}{r_s} + \frac{r_s}{r_s + 2 \times R_w}\right) \times R_{SE}$$

in which R_w is the radius of water molecule and R_{SE} is the Stoke–Einstein radius calculated using $R_{SE} = (kT/6D\pi\eta)$, in which k is the Boltzmann constant, and η is the viscosity.

[c] Data from Peck et al. (1994).

2.3. Human epidermal membrane (HEM) preparation

HEM was prepared by heat-separation using split-thickness human skin obtained from skin banks (Peck et al., 1995). A randomly selected HEM (from different donor sources) was mounted between two side-by-side diffusion half-cells (surface area around 0.75 cm^2, cell volume of 2 ml) supported with a Millipore filter (Peck et al., 1993). The stratum corneum side faced the donor chamber, and the viable epidermis side faced the receiver chamber. The donor and receiver chambers contained PBS with 0.02% NaN_3. A four-electrode potentiostat system (JAS Instrumental Systems, Inc., Salt Lake City, UT) was used to determine the electrical resistance of HEM using Ohm's law (Li et al., 2001). Only HEM with initial

electrical resistance of >15 kΩ cm^2 was used in the present study. HEM was equilibrated in the diffusion cell at 37 °C for 12 h to establish constant HEM electrical resistance before the start of an experiment. The electrical resistance of HEM generally did not change more than 50% during this 12-h equilibration period. After equilibration, HEM maintained stable electrical resistance for several days (Peck et al., 1993).

2.4. Constant current dc iontophoresis

A 0.27 mA/cm^2 constant current dc was applied with Phoresor II Auto constant current iontophoretic devices (Model No. PM 850, Iomed, Inc., Salt Lake City, UT) using Ag/AgCl and Ag as the driving electrodes at 37 °C for approximately 7 h. The anode was in the donor chamber and cathode was in the receiver chamber. During iontophoresis, the voltage drop across HEM was monitored by reference Ag/AgCl electrodes and calomel electrodes in the PBS and dextran sulfate experiments, respectively (Li et al., 2001, 2003). The electrical resistance of HEM during iontophoresis was determined by the electrical current and the voltage drop across HEM using Ohm's law. Except in the experiments involving dextran sulfate, all experiments were conducted with PBS in both chambers. In the experiments with dextran sulfate, PBS and 1.67% dextran sulfate were the solutions in the donor and receiver chambers, respectively. At the start of the experiment, trace amounts of the radiolabelled permeants were pipetted into the donor chamber (final concentrations: 1000–8000, 500–8000, 400–3000, and 400–6000 dpm/μl for [^{3}H]mannitol, [^{14}C]mannitol, [^{14}C]urea, and [^{14}C]TEA, respectively). In the experiments with PBS, 1 ml samples were taken from the receiver chamber and replaced with the fresh PBS solution at predetermined time intervals (around every 0.5–1 h). In the experiments with dextran sulfate, the entire receiver solution was taken and replaced with fresh dextran sulfate solution at predetermined time intervals. 10 μl samples were also withdrawn from the donor chamber every 1–2 h during the experiment. The entire donor solution was replaced when the concentration of any species had changed by more than 15% due to ion transport and/or the formation of electrochemical reaction products at the electrode (this was estimated to be at 3–4 h into the experiment). The samples were mixed with 10 ml of scintillation cocktail (Ultima Gold^{TM}, Packard Instrument Company, Meriden, CT) and assayed by a liquid scintillation counter (Packard TriCarb^{TM} Model 1900TR Liquid Scintillation Analyzer). Calibration standards of radiolabelled permeants were prepared in PBS and dextran sulfate solution. The instantaneous flux (J) of the permeant between two time points was determined by

$$J = \frac{1}{A}\frac{\Delta Q}{\Delta t} \tag{1}$$

and the apparent instantaneous permeability coefficient (P) of the permeant by

$$P = \frac{1}{C_d A}\frac{\Delta Q}{\Delta t} \tag{2}$$

where Q is the cumulative amount transported across the membrane into the receiver chamber, t is time, A is the diffusional surface area, and C_d is the donor chamber concentration of the permeant. Hence, the permeability coefficient is defined as flux normalized by the concentration C_d.

All iontophoresis experiments were carried out with a dual-permeant experimental design. In these dual-permeant experiments, ^{3}H and ^{14}C labeled permeants were employed in the iontophoresis run, and the transport behaviors of one permeant could be easily compared to that of another. This simultaneous determination of the transport of two permeants through the same HEM sample reduced the influence of HEM sample-to-sample variability in data interpretation.

2.5. Theory and analysis

The flux of an ionic species (J_i) is related to the current density carried by the ion (I_i) as

$$I_i = J_i z_i F \tag{3}$$

where F is the Faraday's constant and z_i is the valence of charge. For electrophoresis dominant transport during iontophoresis, the permeability coefficient of an ionic permeant (P_i) can be expressed by

$$P_i = \varepsilon \frac{z_i F D_i H_i}{R_{gas} T}\frac{\Delta\varphi}{\Delta x} \tag{4}$$

where ε is the combined membrane porosity and tortuosity factor, $\Delta\varphi$ is the average electrical potential across the membrane, Δx is the effective membrane

thickness, D_i is the free diffusion coefficient of the permeant provided in Table 1, R_{gas} is the gas constant, T is the absolute temperature, and H_i is the hindrance factor for diffusion. The hindrance factor, H_i, is a function of membrane pore size and permeant size. Assuming cylindrical pore geometry in the membrane and using the asymptotic centerline approximation, the hindrance factor can be expressed as (Deen, 1987)

$$H_i = \frac{6\pi(1-\lambda_i)^2}{K_t} \tag{5}$$

where λ_i is the ratio of the permeant hydrated radius, r_s (Table 1), to pore radius, R_p,

$$K_t = \frac{9}{4}\pi^2\sqrt{2}(1-\lambda_i)^{-2.5}\left[1+\sum_{n=1}^{2}a_n(1-\lambda_i)^n\right] + \sum_{n=0}^{4}a_{n+3}\lambda_i^n$$

and $a_1 = -1.217$, $a_2 = 1.534$, $a_3 = -22.51$, $a_4 = -5.612$, $a_5 = -0.3363$, $a_6 = -1.216$, $a_7 = 1.647$. When λ_i is <0.4, Eq. (5) is equivalent to the commonly used Renkin equation. For electroosmotic transport of a neutral permeant during iontophoresis and at the convection limit (the convection limit assumption will be assessed later in Section 3), the apparent permeability coefficient for the neutral permeant (P_N) can be expressed by

$$P_N = \varepsilon W_N v \tag{6}$$

where W_N is the hindrance factor for convection and v is the effective linear solvent flow velocity due to electroosmosis. W_N is a function of the membrane pore size and permeant radius. With the same assumptions stated for Eq. (5),

$$W_N = \frac{(1-\lambda_N)^2(2-(1-\lambda_N)^2)K_s}{2K_t} \tag{7}$$

where λ_N is the ratio of the hydrated radius of the permeant molecule to the pore radius,

$$K_s = \frac{9}{4}\pi^2\sqrt{2}(1-\lambda_N)^{-2.5}\left[1+\sum_{n=1}^{2}b_n(1-\lambda_N)^n\right] + \sum_{n=0}^{4}b_{n+3}\lambda_N^n$$

and $b_1 = 0.1167$, $b_2 = -0.04419$, $b_3 = 4.018$, $b_4 = -3.979$, $b_5 = -1.922$, $b_6 = 4.392$, $b_7 = 5.006$. K_t has the same expression as that in Eq. (5). The effective flow velocity, v, is proportional to the electric field (Sims et al., 1993) and can be expressed as

$$v = k_\sigma \frac{\Delta\varphi}{\Delta x} \tag{8}$$

where $\Delta\varphi/\Delta x$ is the average electrical potential gradient across the membrane. k_σ is the electric field normalized convective solvent flow velocity parameter that is a function of the effective pore charge density and the pore size of the HEM pores (Sims et al., 1993). If pore radius $\gg$ Debye–Huckel thickness, the electroosmotic velocity can be written as

$$v = \frac{\sigma}{\kappa\eta}\left(\frac{\Delta\varphi}{\Delta x}\right) \tag{9}$$

where σ is the pore charge density, $1/\kappa$ is the Debye–Huckel thickness, and η is the viscosity of the solution in the pore (Sims et al., 1991). At this point it should be mentioned that according to Eqs. (6) and (8), it is also important to note that variability of membrane permeability coefficients of neutral permeants is relatively independent to ε during constant current iontophoresis because $\varepsilon(\Delta\varphi/\Delta x)$ is generally invariant at constant current (also see Eq. (4)). From this it would follow that the flux variability of polar neutral permeant transport during iontophoresis should be mainly dependent on the HEM effective pore charge parameter (k_σ) and effective pore size (W_N). Possible pore charge distributions (i.e. porosity of the negatively charged pores for electroosmosis versus total porosity; Li et al., 1999) are embedded in k_σ.

Combining Eqs. (3), (4) and (6), the ratio of permeability coefficient of a neutral permeant (P_N) to the total current density I is

$$\frac{P_N}{I} = \frac{W_N v R_{gas} T}{F^2(\Delta\varphi/\Delta x)\sum C_j D_j z_j^2 H_j} \tag{10}$$

where $\sum C_j D_j z_j^2 H_j$ is the summation of the contribution for all background electrolyte ions in the solution to the total current density $\left(I = \sum I_j\right)$. The ratio of permeability coefficient of an ionic permeant (P_i) to the total current density is

$$\frac{P_i}{I} = \frac{D_i z_i H_i}{F\sum C_j D_j z_j^2 H_j} \tag{11}$$

From Eqs. (10) and (11), the permeability coefficient of a neutral permeant (P_N) with respect to that of an ionic permeant (P_i) at the same time point in an iontophoresis run can be expressed as

$$P_N = \frac{W_N v R_{gas} T}{F(\Delta\varphi/\Delta x) D_i z_i H_i} P_i \quad (12)$$

Eq. (12) can be simplified to

$$P_N = c_1 \frac{k_\sigma W_N}{H_i} P_i \quad (13)$$

where c_1 is a constant.

From Eq. (10), the relationship between the permeability coefficient of one neutral permeant with respect to that of another at the same time point in an iontophoresis run can be expressed as

$$P_{N,a} = \frac{W_{N,a}}{W_{N,b}} P_{N,b} \quad (14)$$

where the subscripts a and b refer to neutral permeants a and b, respectively. From Eq. (6), the relative time-dependent change in the permeability coefficient of one neutral permeant with respect to that of another permeant from time point 1 to time point 2 during iontophoresis can be expressed as

$$\frac{(\Delta P_{N,a})/P_{N,a}}{(\Delta P_{N,b})/P_{N,b}} = \frac{(W_{N,a,2}k_{\sigma,2}/W_{N,a,1}/k_{\sigma,1}) - 1}{(W_{N,b,2}k_{\sigma,2}/W_{N,b,1}/k_{\sigma,1}) - 1} \quad (15)$$

where the subscripts 1 and 2 refer to time points 1 and 2, respectively. Eqs. (12), (14) and (15) were the main equations used to analyze the data obtained in the present study.

In the present study, only the data obtained after 2 h into the iontophoresis run were used in data analysis. The 2-h time point was chosen for two reasons. First, the passive transport lag time for electric field altered HEM was determined to be less than 1 h (Song et al., 2002). Since electroosmosis enhancement would reduce transport lag time by around two-fold at 1–2 V, any changes in permeability coefficients observed after 2 h into the iontophoresis run should be primarily attributed to changes occurring in the transport properties of HEM (lag time enhancement calculations were performed using the equation of Kasting, 1992 and the enhancement factor data from Li et al., 1998). Second, the current FDA approved non-invasive iontophoresis glucose monitoring system uses a 2-h warm-up period.

3. Results and discussion

3.1. Mannitol and TEA dual permeant experiments

The mannitol and TEA data of the 0.27 mA/cm^2 constant current dc iontophoresis experiments with HEM in PBS are presented in Table 2. The mannitol and TEA permeability coefficients at around 2 h into the iontophoresis run are presented in the second and fourth columns, respectively. The drifts of permeability coefficients of mannitol and TEA in the iontophoresis run from 2 h to the end of the run are presented in the third and fifth columns, respectively. Three notable conclusions are observed in Table 2. First, the average mannitol permeability coefficients (electroosmotic transport) were approximately 5% to those of TEA (combined electrophoretic and electroosmotic transport). This result is consistent with the previously established flux enhancement due to electroosmosis and electrophoresis in iontophoretic transport across HEM (Sims et al., 1991; Zhu et al., 2001). The data in Table 2 also show significantly lower inter-sample variability for TEA (CV = 23%) than that for mannitol (CV = 65%) ($p < 0.01$, F-test for the equality of variance). In addition to the inter-sample variability, the time-dependent changes of the permeability coefficients during iontophoresis (i.e. permeability drifts) for TEA (average = 14%) are also less than those for mannitol (average = 40%). The different magnitudes of the inter-sample variability and the different extent of time-dependent changes in permeability for the model ionic and neutral permeants suggest the hypotheses that: (a) electric field induced alterations of the properties (e.g. the effective pore size) of the predominant transport pathways for ionic and neutral permeants are different, and (b) electroosmosis variability is responsible for the rather large observed transdermal iontophoretic flux variability of polar non-electrolytes such as mannitol.

To further examine these hypotheses, the correlation between the permeability coefficients of mannitol and TEA was analyzed. The sixth and seventh columns in Table 2 show the linear least squares regression slopes and the correlation coefficients between the permeability coefficients of mannitol and TEA obtained in each individual HEM iontophoresis run. Fig. 1 summarizes the mannitol and TEA data of all time points after 2 h during iontophoresis with a linear regression through

Table 2
Results of 0.27 mA/cm^2 constant current dc iontophoresis with mannitol and TEA

HEM	$P_{mannitol}$ (cm/s)[a]	Fractional change[b]	P_{TEA} (cm/s)[a]	Fractional change[b]	Slope[c]	(r^2)[d]	$P_{mannitol}$ to P_{TEA} ratio[e]
B1	8.9E−8	0.6	1.1E−5	0.3	0.013	0.93	0.008
B2	2.7E−7	1.3	1.2E−5	0.4	0.07	0.93	0.022
B3	3.1E−7	0.5	1.4E−5	0	−0.3	0.47	0.022
B4	5.7E−7	0	1.4E−5	0.2	0.015	0.76	0.041
B5	4.4E−7	−0.1	7.5E−6	0	−0.07	0.18	0.059
B6	7.4E−7	0.2	1.9E−5	−0.2	0.007	0.05	0.039
B7	2.3E−7	0.5	1.1E−5	0.4	0.03	0.91	0.021
B8	1.7E−7	0.3	1.3E−5	0.1	0.03	0.65	0.013
B9	3.4E−7	0.2	1.2E−5	0.1	0.04	0.79	0.028
B10	6.5E−7	0.6	1.3E−5	0.3	0.08	0.90	0.050
B11	1.1E−6	0.2	1.0E−5	0.1	0.2	0.48	0.11
B12	1.2E−6	0.3	7.9E−6	0.4	0.09	0.85	0.15
B13	1.1E−6	0.4	1.2E−5	0.1	0.16	0.68	0.092
B14	9.0E−7	0.4	1.3E−5	0.1	0.19	0.86	0.069
B15	3.2E−7	0.1	1.0E−5	0	0.05	0.75	0.032
Mean (CV)[f]	5.6E−7 (65%)	0.4	1.2E−5 (23%)	0.1	0.043 (290%)		0.050 (80%)

[a] Permeability coefficient at 2 h.
[b] Fraction of permeability coefficient change: $(P_{end} - P_{2h})/P_{2h}$, where P_{2h} is the permeability coefficient at 2 h and P_{end} is the permeability coefficient at the end of the experiment (7 h).
[c] Linear least squares slope of $P_{mannitol}$ vs. P_{TEA} from 2 h to the end of the experiment with variable y-intercept.
[d] Correlation coefficient r^2 of the linear least squares slope.
[e] Ratio of permeability coefficient of mannitol to that of TEA at 2 h.
[f] Mean and coefficient of variation (CV) of the data of all HEM samples.

the origin. The r^2 value in the figure is calculated according to Zar (1999). In Table 2, although 6 out of 15 iontophoresis runs show a reasonably good correlation between the permeability coefficients of mannitol and TEA within a run ($r^2 > 0.8$), the large variability of the linear least squares slopes among the HEM samples (slope = 0.043 ± 0.126, mean ± S.D.) and the large data scatter in Fig. 1 show no general correlation

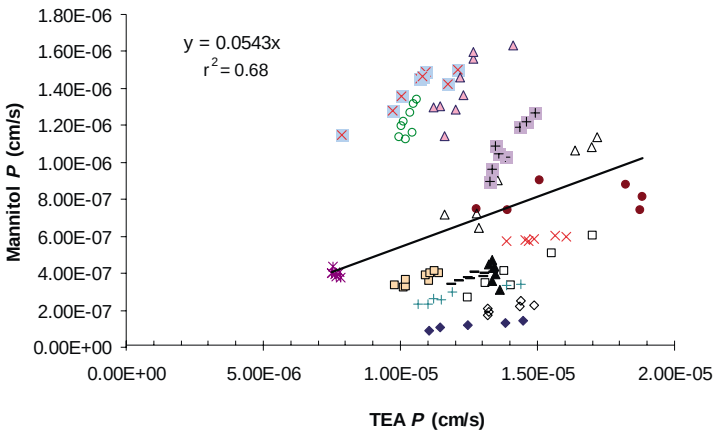

Fig. 1. Relationship between the permeability coefficients (P) of mannitol and TEA in dual-permeant experiments of 0.27 mA/cm^2 constant current dc iontophoresis. The line is the linear least squares line through the origin for the data. Each symbol represents an individual iontophoresis run of the 15 experiments. Each data point represents an individual sampling point during iontophoresis.

between mannitol and TEA permeability coefficients among different HEM samples. This further supports the hypothesis that flux variabilities of ionic permeants are not related to those of the neutral permeants, and this is likely due to the different iontophoretic transport mechanisms of the ionic and neutral permeants (i.e. electrophoresis as the dominant transport mechanism versus electroosmosis, respectively). Therefore, the flux of an ionic permeant cannot be used to accurately predict the flux of a neutral permeant during constant current iontophoresis even when the permeants have similar molecular sizes (poor correlation between the mannitol and TEA data in Fig. 1). The large variability of the permeability coefficient ratios of mannitol to TEA at the 2-h time point into the iontophoresis run (the last column in Table 2) also illustrates this point.

3.2. Flux variability and iontophoretic transport mechanisms

During constant current dc iontophoresis in the present study, because the total current was maintained constant (by adjusting the applied voltage across HEM) and trace amounts of the permeant were used, the total flux of the background electrolyte ions (e.g. sodium and chloride ions) was maintained constant. The inter-sample variability and the time-dependent changes in the permeability for TEA during iontophoresis were therefore mainly a result of the different transport hindrances experienced by TEA and the background electrolyte ions (Eq. (11)). These pore size effects corresponded to a three-fold range in the variabilities of ionic permeants (7E−6 to 1.9E−5 cm/s, Table 2) when the permeant size was about two times larger than those of the background electrolyte (Table 1). The three-fold range is consistent with the results in a recent study demonstrating the effects of background electrolyte ion sizes upon the predictability of the Nernst–Planck theory (Zhu et al., 2001). To summarize, flux variabilities were observed with TEA, but they were generally not very great (compared to mannitol) because (a) TEA and background electrolyte ions follow the same transport mechanism and (b) the molecular size of TEA are within a factor of two of those of the background electrolyte ions. Flux variabilities of TEA were therefore not further characterized in the present study.

In contrast to the results obtained with TEA for which changes in the effective pore size alone during constant current iontophoresis is believed to account for the flux variability, iontophoretic transport of mannitol is governed by the effective pore size and the effective pore charge density of the negatively charged pores responsible for electroosmotic transport in HEM (Peck et al., 1996; Li et al., 1999; Pikal, 2001). Inter-sample flux variabilities and flux drifts during iontophoresis based on the effective pore size and effective pore charge of HEM were therefore further investigated in the following mannitol/urea experiments.

3.3. Mannitol and urea dual permeant experiments

Table 3 presents the mannitol and urea data of the 0.27 mA/cm^2 constant current dc iontophoresis experiments with HEM in PBS. The second and fourth columns in Table 3 show, respectively, the permeability coefficients of mannitol and urea at 2 h into the iontophoresis run. The permeability coefficients of urea on average are approximately 2.5 times greater than those of mannitol. This is consistent with the previous finding of hindered electroosmotic transport with effective pore radii of around 0.6–0.9 nm (Li et al., 1998). Another observation that can be made in Table 3 is the essentially same permeability drifts of mannitol and urea (presented in the third and fifth columns in Table 3, respectively). A ±15% difference between the permeability drifts of mannitol and urea is considered to be within experimental error in transport experiments in general (unpublished data in transport experiments with synthetic membranes). The parallel permeability increase of urea and mannitol with time during iontophoresis is consistent with the effective pore charge density being a main factor responsible for the time-dependent flux variability observed with the neutral permeants during constant current iontophoresis. The last three columns in Table 3 present the slopes of the linear regressions and the coefficients of determination between mannitol and urea permeability coefficients and the permeability coefficient ratios of mannitol to urea, respectively, of each iontophoresis run. A comparison between the mannitol/TEA permeability coefficient regressions in Table 2 and the mannitol/urea regressions in Table 3 shows better correlations between the mannitol and

Table 3
Results of 0.27 mA/cm^2 constant current dc iontophoresis with mannitol and urea

HEM	$P_{mannitol}$ (cm/s)[a]	Fractional change[b]	P_{urea} (cm/s)[a]	Fractional change[b]	% change of k_σ[c]	R_p (nm)[d]	Slope[e]	(r^2)[f]	$P_{mannitol}$ to P_{urea} ratio[g]
C1	3.0E−7	0.7	8.9E−7	0.2	0	0.63–0.74	0.94	0.92	0.34
C2	3.3E−7	0.1	8.0E−7	0.1	N/A	0.67	0.16	0.67	0.41
C3	1.5E−7	0.7	7.6E−7	0.3	10	0.54–0.58	0.51	0.92	0.20
C4	3.1E−7	1.2	1.0E−6	0.8	60	0.61–0.66	0.51	0.99	0.31
C5	4.2E−7	0.3	8.8E−7	0.1	0	0.73–0.81	1.1	0.86	0.48
C6	2.5E−7	0.4	5.6E−7	0.3	20	0.70–0.74	0.63	0.88	0.45
C7	3.8E−7	0.2	7.1E−7	0.2	N/A	0.78	0.76	0.83	0.54
C8	2.7E−7	0.6	7.6E−7	0.3	20	0.63–0.68	0.74	0.92	0.36
C9	3.1E−7	0.4	7.2E−7	0.2	10	0.70–0.76	0.61	0.97	0.43
C10	4.3E−7	0.6	1.0E−6	0.6	60	0.69	0.39	1.00	0.43
C11	2.6E−7	0.6	9.0E−7	0.5	50	0.59	0.38	0.99	0.29
C12	4.9E−7	0	1.2E−6	0.1	N/A	0.68	0.33	0.68	0.41
C13	1.7E−7	1.3	4.5E−7	1.0	90	0.64–0.67	0.52	0.97	0.38
C14	3.3E−7	1.6	7.1E−7	1.3	120	0.71–0.75	0.59	0.96	0.46
C15	4.4E−7	0.7	1.2E−6	0.7	65	0.64	0.39	0.97	0.37
C16	2.9E−7	0.6	8.8E−7	0.6	60	0.61	0.32	0.92	0.33
Mean (CV)[h]	3.2E−7 (30%)	0.6	8.4E−7 (24%)	0.4			0.56 (44%)		0.39 (22%)

[a] Permeability coefficient at 2 h.
[b] Fraction of permeability coefficient change: $(P_{end} - P_{2h})/P_{2h}$, where P_{2h} is the permeability coefficient at 2 h and P_{end} is the permeability coefficient at the end of the experiment (7 h).
[c] Percent of effective electroosmotic flow velocity change from 2 h to the end of the experiment.
[d] Effective pore radius (R_p) from 2 h to the end of the experiment.
[e] Linear least squares slope of $P_{mannitol}$ vs. P_{urea} from 2 h to the end of the experiment with variable y-intercept.
[f] Correlation coefficient r^2 of the linear least squares slope.
[g] Ratio of permeability coefficient of mannitol to that of urea at 2 h.
[h] Mean and coefficient of variation (CV) of the data of all HEM samples.

urea pairs. This conclusion is deduced from the following. First, only 2 out of 16 samples in Table 3 have $r^2 < 0.8$ (both due to the relatively constant permeability coefficients of mannitol during iontophoresis) versus the 9 out of 15 samples in Table 2. Second, the variability of the linear regression slopes among different samples in Table 3 (mean ± S.D.: 0.56 ± 0.25) is smaller than those in Table 2 (mean ± S.D.: 0.043 ± 0.126). Third, the mannitol-to-urea permeability coefficient ratios at the 2-h iontophoresis time point in Table 3 (mean ± S.D.: 0.39 ± 0.08) show smaller variation than those of the mannitol-to-TEA permeability coefficient ratios in Table 2 (mean±S.D.: 0.05 ± 0.04).

It should be noted that the inter-sample variabilities of mannitol in Table 3 (ranging from 1.5E−7 to 4.9E−7 cm/s, CV: 30%) are less than those observed in Table 2 (from 0.9E−7 to 1.2E−6 cm/s, CV: 65%) ($p < 0.01$, F-test), but the drifts of mannitol permeability coefficients in Table 3 (mean: 60%) are larger than those in Table 2 (mean: 40%). These differences in variabilities prompted the repeats of the mannitol iontophoresis experiments under the same experimental conditions with another set of 16 HEM samples from different skin donors. Table 4 presents the mannitol permeability coefficients and permeability drifts in these experiments. The large inter-sample variability in Table 4 (ranging from 1.6E−7 to 1.7E−6 cm/s, CV: 100%) is similar to that in Table 2 ($p = 0.43$, F-test), and the large permeability drifts during iontophoresis (mean % change: 90%) in Table 4 are similar to those in Table 3. Possible relationships between the initial HEM electrical resistance before iontophoresis application and flux variabilities during iontophoresis were also examined. No general relationship between the variabilities and HEM initial resistance was found among the HEM samples in Tables 2–4 (data not shown).

Table 4
Results of 0.27 mA/cm^2 constant current dc iontophoresis with mannitol

HEM	$P_{mannitol}$ (cm/s)[a]	Fractional change[b]
D1	3.9E−7	0.1
D2	1.6E−7	1.1
D3	2.5E−7	0.5
D4	1.9E−7	0.5
D5	2.1E−7	0.7
D6	2.8E−7	0.6
D7	4.0E−7	0.2
D8	1.9E−7	1.8
D9	4.5E−7	0.2
D10	2.0E−7	2.7
D11	3.1E−7	1.5
D12	1.7E−6	0.4
D13	1.5E−6	0.6
D14	4.3E−7	1.4
D15	3.4E−7	1.2
D16	4.2E−7	0.5
Mean (CV)[c]	4.7E−7 (100%)	0.9

[a] Permeability coefficient at 2 h.
[b] Fraction of permeability coefficient change: $(P_{end} - P_{2h})/P_{2h}$, where P_{2h} is the permeability coefficient at 2 h and P_{end} is the permeability coefficient at the end of the experiment (7 h).
[c] Mean and coefficient of variation (CV) of the data of all HEM samples.

3.4. Effects of effective pore size and effective pore charge during electroosmotic transport

The applied voltage across HEM during constant current dc iontophoresis varied within a single iontophoresis run and among HEM samples. In the present study, the applied voltage during 0.27 mA/cm^2 constant current iontophoresis ranged between 0.7 and 2.8 V. Under these applied voltage conditions, electroosmosis was the dominant transport mechanism and the transport of urea and mannitol approached the convection limit (Li et al., 1998); the errors of the convection limit assumption at 1.7 V (the average) were less than 2 and 8% for mannitol and urea, respectively, and in the worst case scenario (i.e. at 0.7 V), these errors were estimated to be around 13 and 35%, respectively.

The permeability drifts of the neutral permeants within a single iontophoresis run during iontophoresis (third and fifth columns of Table 3) were analyzed based on the effective pore size and k_σ parameters of HEM. Using the ratios of the urea and mannitol permeability coefficients and Eq. (14), the effective pore radii during iontophoresis were determined. The permeability drift data, effective pore radii, and Eq. (15) were then used to determine the percent of increase in k_σ during iontophoresis. These results are shown in the sixth and seventh columns in Table 3. Among the 16 HEM experiments in Table 3, three HEM samples did not show any significant permeability drifts of mannitol and urea ($\leq$20%) during iontophoresis. Three out of 16 HEM samples experienced moderate changes in mannitol permeability coefficients (around 20–50%) during iontophoresis. In these three iontophoresis runs, both the increase in the effective pore size and k_σ are responsible for the permeability drifts during iontophoresis. Ten HEM samples in Table 3 show a larger than 50% change in mannitol permeability coefficients. When there was a large increase in mannitol permeability coefficients, significant increases in k_σ ($\geq$50%) were generally observed (7 out of 10 HEM samples).

Fig. 2 summarizes the mannitol and urea data. It includes all HEM samples and all the time points for each sample after 2 h into the iontophoresis experiments. The figure shows eight- and five-fold variabilities of the permeability coefficients of mannitol and urea, respectively. Also shown in the figure is a linear correlation between the permeability coefficients of mannitol and urea. The line in Fig. 2 represents the linear regression through the origin for the data. According to Eqs. (14) and (15), if the effective pore size during iontophoresis within a single iontophoresis run and among different HEM experiments is constant, k_σ will be primarily responsible for the time-dependent flux drifts and inter-sample flux variability. In this case, the plot of $P_{N,a}$ versus $P_{N,b}$ will show a good linear correlation (a straight line with a constant slope through the origin), yielding a linear least squares slope equal to $W_{N,a}/W_{N,b}$ (Eqs. (10) and (14)). As can be seen in the figure, the mannitol and urea permeability coefficient data form a linear regression line, which are consistent with the large time-dependent electroosmosis increase and inter-sample variability in k_σ during iontophoresis. The vertical deviation (i.e. in the direction of the y-axis) of the data from the linear regression line (within 1.5-fold) can be attributed to pore size variability among different HEM samples as well as pore size variations during iontophoresis. Despite such deviations, the $P_{mannitol}$ versus P_{urea} correlation

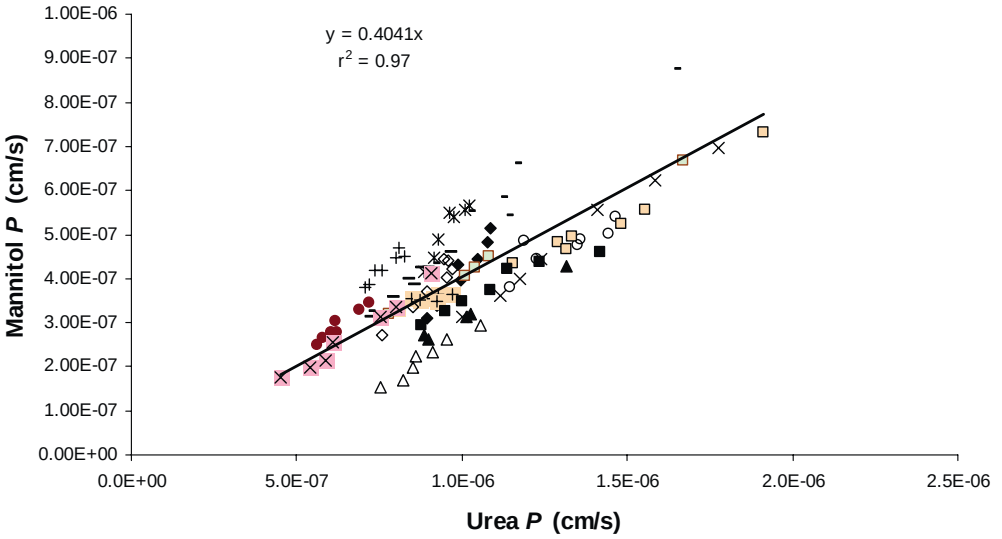

Fig. 2. Relationship between the permeability coefficients (P) of mannitol and urea in dual-permeant experiments of 0.27 mA/cm^2 constant current dc iontophoresis. The line is the linear least squares line through the origin for the data. Each symbol represents an individual iontophoresis run of the 16 experiments. Each data point represents an individual sampling point during iontophoresis.

supports the idea that flux variability of a neutral permeant can be predicted within reasonable accuracy if the flux of another neutral permeant of similar molecular size is known. Examples can be the prediction of phenylalanine iontophoretic permeability coefficients using the permeability coefficients of glucose for the diagnostic test of phenylketonuria in human patients or, vice versa, the prediction of glucose permeability coefficients using those of phenylalanine for blood glucose monitoring in diabetes management. Ongoing studies in our laboratory show a relatively good correlation between the permeability coefficients of phenylalanine and mannitol during iontophoresis with HEM in vitro (data not shown).

3.5. Experiments with high molecular weight dextran sulfate as the background electrolyte in the receiver chamber

The main objective of the experiment with dextran sulfate was to determine the effects of the ion size differences between chloride ion and sodium ion upon flux variability in electroosmotic transport because sodium ion has a larger Stokes–Einstein hydration radius than chloride ion (Table 1). In these experiments, an asymmetric configuration was employed where the receiver solution was 1.67% 500,000 MW dextran sulfate and the donor solution was PBS. With the high molecular weight and hydrophilicity, the dextran sulfate molecules are not expected to alter the pore characteristic of HEM (Hirvonen and Guy, 1997, 1998). Also, the high MW dextran sulfate molecules were not expected to be transported across HEM, so sodium ion was the only conducting ion carrying the current. Under this condition, maintaining a constant current provided constant sodium ion flux across HEM, and sodium ion became the major component in the denominator of Eq. (10). Comparison between the data of the experiments with dextran sulfate and those with PBS allowed the examination of the effects of the size differences of background electrolyte ions upon flux variability.

The mannitol and urea data obtained in the dextran sulfate/PBS asymmetric system are presented in Table 5. Fig. 3 summarizes all mannitol and urea data at all time points (after 2 h into the iontophoresis runs) in the experiments. The correlation between mannitol and urea permeability coefficients in Fig. 3 supports the proposed method of using the permeability coefficient of one neutral permeant to predict the permeability of another neutral permeant during iontophoresis. Having sodium ion as the only current carrier across

Table 5
Results of 0.27 mA/cm^2 constant current dextran sulfate iontophoresis experiments with mannitol and urea

HEM	$P_{mannitol}$ (cm/s)[a]	Fractional change[b]	P_{urea} (cm/s)[a]	Fractional change[b]	% change of k_σ[c]	R_p (nm)[d]	Slope[e]	(r^2)[f]	$P_{mannitol}$ to P_{urea} ratio[g]
E1	2.4E−7	0.3	8.3E−7	0.4	30	0.59	0.23	0.96	0.29
E2	3.6E−7	1.1	1.5E−6	0.6	45	0.56–0.6	0.36	0.96	0.24
E3	2.8E−7	0.6	1.1E−6	0.5	50	0.57	0.41	0.94	0.25
E4	8.9E−8	1.2	2.3E−7	1.3	120	0.65	0.38	0.98	0.39
E5	3.6E−7	0.4	1.2E−6	0.2	10	0.60–0.63	0.59	0.87	0.30
E6	1.9E−7	0.9	8.8E−7	0.5	40	0.55–0.58	0.30	0.91	0.22
E7	4.6E−7	−0.1	1.2E−6	0	N/A	0.65	0.59	0.68	0.38
E8	3.9E−7	0.4	1.5E−6	0.4	40	0.58	0.27	0.94	0.26
E9	2.7E−7	0.2	1.0E−6	0.1	N/A	0.58	0.51	0.81	0.27
E10	4.2E−7	0	1.3E−6	0.2	N/A	0.61	0.17	0.68	0.32
E11	4.2E−7	0	1.5E−6	0.2	N/A	0.59	0.18	0.45	0.28
E12	4.4E−7	0	1.5E−6	0.1	N/A	0.60	0.17	0.84	0.29
E13	3.7E−7	0.8	9.2E−7	0.6	55	0.67–0.70	0.56	0.98	0.40
E14	2.6E−7	0.7	5.9E−7	0.7	65	0.70	0.49	1.0	0.44
E15	7.9E−7	0.3	1.3E−6	0.2	25	0.85	0.57	0.97	0.61
Mean (CV)[h]	3.6E−7 (45%)	0.5	1.1E−6 (33%)	0.4			0.38 (42%)		0.33 (31%)

[a] Permeability coefficient at 2 h.
[b] Fraction of permeability coefficient change: $(P_{end} - P_{2h})/P_{2h}$, where P_{2h} is the permeability coefficient at 2 h and P_{end} is the permeability coefficient at the end of the experiment (7 h).
[c] Percent of effective electroosmotic flow velocity change from 2 h to the end of the experiment.
[d] Effective pore radius (R_p) from 2 h to the end of the experiment.
[e] Linear least squares slope of $P_{mannitol}$ vs. P_{urea} from 2 h to the end of the experiment with variable y-intercept.
[f] Correlation coefficient r^2 of the linear least squares slope.
[g] Ratio of permeability coefficient of mannitol to that of urea at 2 h.
[h] Mean and coefficient of variation (CV) of the data of all HEM samples.

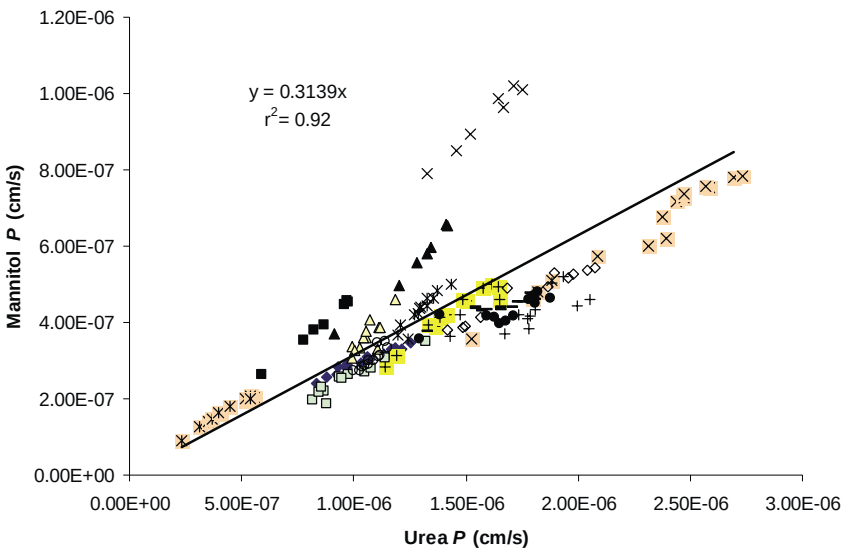

Fig. 3. Relationship between the permeability coefficients (P) of mannitol and urea in dual-permeant experiments of 0.27 mA/cm^2 constant current dc iontophoresis with the dextran sulfate/PBS asymmetric system. The line is the linear least squares line through the origin for the data. Each symbol represents an individual iontophoresis run of the 15 experiments. Each data point represents an individual sampling point during iontophoresis.

HEM did not affect the time-dependent changes in permeability coefficients (third and fifth columns of Table 5) and the inter-sample variability (second and fourth columns) of mannitol and urea. Zhu et al. (2001) have shown the effects of background electrolyte sizes upon the flux variability of ionic permeants. However, the present results show no relationship between flux variability of the neutral permeants and background electrolyte ion size. This again is consistent with the transport mechanisms being different for ions and neutral permeants. In Table 5, similar to the results of Table 3 (in mannitol/urea experiments in PBS) are the essentially same percent of time-dependent permeability increase of mannitol and urea (third and fifth columns) and the essentially same ratios of permeability coefficients of mannitol to those of urea at 2 h (last column). When sodium ion was the only current carrier, 5 out of 15 HEM samples did not show significant permeability drifts of mannitol ($\leq$20%) in Table 5. Four out of 15 samples showed mannitol permeability drifts between around 20 and 50%, and the rest (6 out of 15) showed greater than 50% permeability increase during the iontophoresis runs. Among these 10 HEM iontophoresis runs, the permeability drifts of all but three samples are interpreted to be essentially entirely from time-dependent increases of k_σ during iontophoresis. The increases in effective HEM pore size and in k_σ were important for the permeability drifts observed with the three samples. These results strengthen the conclusion of (time-dependent increase) k_σ being the main factor in the significant permeability drifts of mannitol and urea during constant current iontophoresis.

A separate iontophoresis study with the dextran sulfate/PBS asymmetric system using mannitol and calcium ion as the model permeants was also conducted (data not shown). Calcium ion was used instead of TEA ion because of the availability of calcium ion in serum and its possible therapeutic use (Szanto and Papp, 1998). In this study, the transport data of mannitol and calcium were found to be consistent with those of the mannitol and TEA data in Table 2. Large permeability drifts during iontophoresis were observed with mannitol but not with calcium ion. These results are consistent with the absence of a correlation between the flux variability of ionic and neutral permeants during transdermal iontophoresis.

4. Conclusion

During constant current dc iontophoresis, flux variability is a result of the electric field-induced alteration of the barrier properties of HEM; more specifically, flux variability comes about from the changes in the HEM pore characteristics such as effective pore size and pore charge density that impact upon the transport of the permeant of interest and the background electrolyte ions. It was found that inter-sample variability and time-dependent flux drifts during iontophoresis for ionic permeants were less than those for neutral permeants. This observation is consistent with the hypothesis that such differences in variability and flux drifts were primarily related to the different mechanisms of iontophoretic transport for ionic and neutral permeants (electrophoresis and electroosmosis, respectively). For neutral permeants, the increase of electroosmosis resulting from the changes in the effective pore charge of the HEM pores during iontophoresis was a major factor for the inter-sample variability and the significant flux drifts observed. The exclusion of chloride ion as conducting ion across HEM by using high molecular weight dextran sulfate as the only background electrolyte at the cathode did not reduce inter-sample flux variability and flux drift for neutral permeants during iontophoresis; this is believed to be again related to the mechanisms being different for ionic and neutral permeants.

Acknowledgements

This research was supported by NIH Grant GM063559. The authors thank Mark R. Liddell, Matthew S. Hastings, Guang Yan, Dr. Aniko Szabo, and Dr. David J. Miller for their help. The authors also thank Watson Laboratories, Inc.-Utah for donating some of the skin samples used in the present study.

References

Bath, B.D., Scott, E.R., Phipps, J.B., White, H.S., 2000. Scanning electrochemical microscopy of iontophoretic transport in hairless mouse skin. Analysis of the relative contributions of diffusion, migration, and electroosmosis to transport in hair follicles. J. Pharm. Sci. 89, 1537–1549.

Beck, R.E., Schultz, J.S., 1972. Hindrance of solute diffusion within membranes as measured with microporous membranes of known pore geometry. Biochim. Biophys. Acta 255, 273–303.

Chang, S.L., Hofmann, G.A., Zhang, L., Deftos, L.J., Banga, A.K., 2000. Transdermal iontophoretic delivery of salmon calcitonin. Int. J. Pharm. 200, 107–113.

Deen, W.M., 1987. Hindered transport of large molecules in liquid-filled pores. AIChE J. 33, 1409–1425.

Degim, I.T., Ilbasmis, S., Dundaroz, R., Oguz, Y., 2003. Reverse iontophoresis: a non-invasive technique for measuring blood urea level. Pediatr. Nephrol. 18, 1032–1037.

Hirvonen, J., Guy, R.H., 1997. Iontophoretic delivery across the skin: electroosmosis and its modulation by drug substances. Pharm. Res. 14, 1258–1263.

Hirvonen, J., Guy, R.H., 1998. Transdermal iontophoresis: modulation of electroosmosis by polypeptide. J. Control. Release 50, 283–289.

Kasting, G.B., 1992. Theoretical models for iontophoretic delivery. Adv. Drug Deliv. Rev. 9, 177–199.

Li, S.K., Ghanem, A.H., Peck, K.D., Higuchi, W.I., 1998. Characterization of the transport pathways induced during low to moderate voltage iontophoresis in human epidermal membrane. J. Pharm. Sci. 87, 40–48.

Li, S.K., Ghanem, A.H., Higuchi, W.I., 1999. Pore charge distribution considerations in human epidermal membrane electroosmosis. J. Pharm. Sci. 88, 1044–1049.

Li, S.K., Ghanem, A.H., Teng, C.L., Hardee, G.E., Higuchi, W.I., 2001. Iontophoretic transport of oligonucleotides across human epidermal membrane: a study of the Nernst–Planck model. J. Pharm. Sci. 90, 915–931.

Li, S.K., Higuchi, W.I., Zhu, H., Kern, S.E., Miller, D.J., Hastings, M.S., 2003. In vitro and in vivo comparisons of constant resistance AC iontophoresis and DC iontophoresis. J. Control. Release 91, 327–343.

Lide, D.R., 1990. Handbook of Chemistry and Physics, 71st ed. CRC Press, Boca Raton.

Liu, P., Nightingale, J.A.S., Kurihara-Bergstrom, T., 1993. Variation of human skin permeation in vitro: ionic vs. neutral compounds. Int. J. Pharm. 90, 171–176.

Lopez, R.F., Bentley, M.V., Delgado-Charro, M.B., Guy, R.H., 2001. Iontophoretic delivery of 5-aminolevulinic acid (ALA): effect of pH. Pharm. Res. 18, 311–315.

Marro, D., Kalia, Y.N., Delgado-Charro, M.B., Guy, R.H., 2001. Contributions of electromigration and electroosmosis to iontophoretic drug delivery. Pharm. Res. 18, 1701–1708.

Nicoli, S., Rimondi, S., Colombo, P., Santi, P., 2001. Physical and chemical enhancement of transdermal delivery of triptorelin. Pharm. Res. 18, 1634–1637.

Peck, K.D., Ghanem, A.H., Higuchi, W.I., Srinivasan, V., 1993. Improved stability of the human epidermal membrane during successive permeability experiments. Int. J. Pharm. 98, 141–147.

Peck, K.D., Ghanem, A.H., Higuchi, W.I., 1994. Hindered diffusion of polar molecules through and effective pore radii estimates of intact and ethanol treated human epidermal membrane. Pharm. Res. 11, 1306–1314.

Peck, K.D., Ghanem, A.H., Higuchi, W.I., 1995. The effect of temperature upon the permeation of polar and ionic solutes through human epidermal membrane. J. Pharm. Sci. 84, 975–982.

Peck, K.D., Srinivasan, V., Li, S.K., Higuchi, W.I., Ghanem, A.H., 1996. Quantitative description of the effect of molecular size upon electroosmotic flux enhancement during iontophoresis for a synthetic membrane and human epidermal membrane. J. Pharm. Sci. 85, 781–788.

Phipps, J.B., Gyory, J.R., 1992. Transdermal ion migration. Adv. Drug Deliv. Rev. 9, 137–176.

Pikal, M.J., 2001. The role of electroosmotic flow in transdermal iontophoresis. Adv. Drug Deliv. Rev. 46, 281–305.

Sieg, A., Guy, R.H., Delgado-Charro, M.B., 2003. Reverse iontophoresis for noninvasive glucose monitoring: the internal standard concept. J. Pharm. Sci. 92, 2295–2302.

Sims, S.M., Higuchi, W.I., Srinivasan, V., 1991. Interaction of electric field and electroosmotic effects in determining iontophoretic enhancement of anions and cations. Int. J. Pharm. 77, 107–118.

Sims, S.M., Higuchi, W.I., Srinivasan, V., Peck, K.D., 1993. Ionic partition coefficients and electroosmotic flow in cylindrical pores: comparison of the predictions of the Poisson–Boltzmann equation with experiment. J. Colloid Interface Sci. 155, 210–220.

Singh, P., Anliker, M., Smith, G.A., Zavortink, D., Maibach, H.I., 1995. Transdermal iontophoresis and solute penetration across excised human skin. J. Pharm. Sci. 84, 1342–1346.

Smyth, H.D., Becket, G., Mehta, S., 2002. Effect of permeation enhancer pretreatment on the iontophoresis of luteinizing hormone releasing hormone (LHRH) through human epidermal membrane (HEM). J. Pharm. Sci. 91, 1296–1307.

Song, Y., Li, S.K., Peck, K.D., Zhu, H., Ghanem, A.H., Higuchi, W.I., 2002. Human epidermal membrane constant conductance iontophoresis: alternating current to obtain reproducible enhanced permeation and reduced lag times of a nonionic polar permeant. Int. J. Pharm. 232, 45–57.

Szanto, Z., Papp, L., 1998. Effect of the different factors on the iontophoretic delivery of calcium ions from bentonite. J. Control. Release 56, 239–247.

Tamada, J.A., Garg, S., Jovanovic, L., Pitzer, K.R., Fermi, S., Potts, R.O., 1999. Noninvasive glucose monitoring: comprehensive clinical results. JAMA 282, 1839–1844.

Tierney, M.J., Tamada, J.A., Potts, R.O., Jovanovic, L., Garg, S., 2001. Clinical evaluation of the GlucoWatch biographer: a continual, non-invasive glucose monitor for patients with diabetes. Biosens. Bioelectron. 16, 621–629.

Zar, J.H., 1999. Biostatistical Analysis, 4th ed. Prentice-Hall, New Jersey.

Zhu, H., Peck, K.D., Li, S.K., Ghanem, A.H., Higuchi, W.I., 2001. Quantification of pore induction during iontophoresis with human epidermal membrane: the importance of background electrolyte selection. J. Pharm. Sci. 90, 932–942.

Zhu, H., Li, S.K., Peck, K.D., Miller, D.J., Higuchi, W.I., 2002. Improvement on conventional constant current DC iontophoresis: a study using constant conductance AC iontophoresis. J. Control. Release 82, 249–261.